Origin and growth of peroxisomes in yeast

Yuan, Wei

Chapter 2

Saccharomyces cerevisiae pex3 cells contain preperoxisomal membrane vesicles

Yuan Wei, Arjen M. Krikken, and Ida J. van der Klei

Molecular Cell Biology, Groningen Biomolecular Sciences and Biotechnology Institute (BBA) University of Groningen, PO Box 11103, 9300 CC Groningen, The Netherlands

Abstract

We demonstrated that *Saccharomyces cerevisiae pex3* cells contain vesicular peroxisomal membrane structures. These structures are relatively stable and harbor the peroxisomal receptor docking protein Pex14 in conjunction with Pex8. Pex11 was mislocalized to mitochondria, whereas the other tested peroxisomal membrane proteins were below the limit of detection. Upon reintroduction of Pex3 in cells lacking Pex3 protein, the Pex14 containing vesicles matured into functional peroxisomes, suggesting that the vesicles are preperoxisomal structures.

Introduction

Peroxisomes are ubiquitous multifunctional organelles that are present in almost all eukaryotic cells. Their functions vary with the organism in which they occur and with their developmental stage. Common functions include hydrogen peroxide metabolism and β-oxidation of fatty acids (van den Bosch et al., 1992).

Peroxisome numbers are highly flexible. Organelle abundance enhances upon stimulation of peroxisome proliferation, but deceases upon induction of pexophagy (autophagic degradation of peroxisomes) (Honsho et al.; Mast et al., 2015; Smith and Aitchison, 2013).How organelle numbers increase is still a matter of debate. For yeast, two main machineries of peroxisome development have been documented (Lazarow and Fujiki, 1985; Tabak et al., 2008, 2013). The first one prescribes that peroxisomes, as semi-autonomous organelles, proliferate by growth and fission. Related to this, multiple components involved in organelle fission and inheritance have been firmly established (Opaliński et al., 2011, 11; Motley et al., 2008; Williams et al., 2015).

Alternatively, peroxisomes may form from the endoplasmic reticulum (ER), which involves sorting of peroxisomal membrane proteins (PMPs) to the ER, followed by Pex3/Pex19 dependent vesicle formation and Pex1/Pex6 mediated vesicle fusion (van der Zand et al., 2012). This model is pre-dominantly based on the analysis of organelle formation in yeast *pex3* deletion strains upon re-introduction of the missing *PEX3* gene (Hoepfner et al., 2005) and supported by data indicating that peroxisomal membrane vesicles can be formed *in vitro* from the ER (Lam et al., 2011; Agrawal., 2016). On the other hand, recent studies indicated that yeast Pex1 and Pex6 are not involved in the fusion of ER-derived PMPs-containing vesicles (Knoops et al., 2015; Motley et al., 2015), but play a role in peroxisomal

matrix protein import in line with earlier reports on the function of these proteins (Grimm et al., 2012).

The ER based model also has been challenged by data obtained in *Hansenula polymorpha* that indicated that *H. polymorpha pex3* cells contain preperoxisomal vesicles (PPVs) that harbor components of the matrix protein docking complex (Pex13, Pex14 and Pex8), but not of the RING complex (Pex2, Pex10, Pex12), thus explaining why a functional importomer is not formed (Knoops et al., 2014). In addition, *H. polymorpha* PPVs lacked the fission protein Pex11 as well as the ATP-AMP transporter Pmp47. Upon re-induction of Pex3, the PPVs, but not the ER, were the target for Pex3 and subsequently matured into normal peroxisomes.

These results prompted us to re-investigate *S. cerevisiae pex3* cells, as these are generally considered to lack peroxisome remnants structures (Hettema et al., 2000; van der Zand et al., 2010). Our data indicate that *S. cerevisiae pex3* cells contain clusters of small membrane vesicles that contained Pex14 and Pex8, but not Pex13, Pex10, Pex11 and Ant1, the homologue of *H. polymorpha* Pmp47. We furthermore show that these vesicles mature into functional peroxisomes upon reintroduction of Pex3, like observed in *H. polymorpha*.

Materials and methods

Strains and growth conditions

The *S. cerevisiae* strains used in this study are derivatives of BY4742 (*his3*Δ1; *leu2*Δ0; *lys2*Δ0; *ura3*Δ0), or DF5 (*trp1*Δ1; *ura*3Δ52; *his*3Δ200; *leu*2Δ3; *lys*2Δ801) and are listed in **Table 1**. *S. cerevisiae* cells were grown at 30°C on either YPD (1% yeast extract, 1% peptone and 1% glucose), selective media containing 0.67% yeast nitrogen base without amino acids (YNB; Difco BD) or mineral medium supplemented with 1% glucose or a mixture of 0.1% glucose and 0.1% oleic acid (MM-O). For

growth on agar plates, the medium was supplemented with 2% agar. For selection of antibiotic resistant transformants, YPD plates containing 200 µg/ml Zeocin (Invitrogen), 200 µg/ml Hygromycin B (Invitrogen) or 100 µg/ml Nourseothricin (Werner Bioagents) were used. For selection of auxotrophic transformants, mineral medium was supplemented with the required amino acids.

Molecular and Biochemical techniques

Oligonucleotides used in this study are listed in **Table 2**. Standard recombinant DNA techniques were performed as described previously (Janke et al., 2004). Preparative polymerase chain reactions (PCR) were carried out with Phusion polymerase (Thermo Scientific). Initial selection of positive transformants by colony PCR was carried out using Phire polymerase (Thermo Scientific). Extracts prepared from cells treated with 12.5% trichloroacetic acid were prepared for SDS-polyacrylamide gel electrophoresis and Western blotting (WB) as detailed previously (Baerends et al., 2000). Equal amounts of proteins were loaded per lane. Blots were probed with rabbit polyclonal antisera against Pex14, pyruvate carboxylase-1 (Pyc1) or glucose-6-phosphate dehydrogenase (G6PD). mGFP-fusion proteins of Pex10, Pex11, Pex13, Ant1 were probed with mouse monoclonal antiserum against green fluorescence protein (GFP; Santa Cruz Biotechnology, sc-9996). Pyc1 and G6PD were used as loading controls. Secondary antibodies conjugated to horseradish peroxidase were used for detection.

Construction of *pex3* Pex14-mGFP, *pex3 atg1* Pex14-mGFP and *pex3 atg1* Pex14-6xHA strains

The *S. cerevisiae pex3* strain was obtained from the Euroscarf collection (**Table 1**). The *PEX3* deletion was confirmed by colony PCR with primers TER202 and TER203.

ATG1 was disrupted by replacing the *ATG1* region with the nourseothricin (Nat) resistance gene using a PCR fragment containing the selective marker and 50bp of *ATG1* flanking regions. The PCR fragment was amplified with the primers TER208 and TER209 using plasmid pAG25 (Goldstein and McCusker, 1999) as a template, and then transformed into *pex3* cells. Nourseothricin resistant transformants were selected and the correct integration was checked by colony PCR using the primers TER210 and TER211, and confirmed by Southern blotting.

To obtain *pex3* Pex14-mGFP and *pex3 atg1* Pex14-mGFP, a fragment containing *PEX14-mGFP* was amplified using primers TER216 and TER217 from the yeast Euroscarf GFP fusion collection and transformed into *pex3* and *pex3 atg1* cells, respectively. Subsequently, correct integration of *PEX14-mGFP* was confirmed by colony PCR using TER198 and TER199.

Construction of *pex3 atg1* strains for co-localization studies

A fragment encoding *mCherry* was cloned from plasmid pARM001 (Kumar et al., 2016) using primers TER214 and TER215, and then transformed into BY4742 and *pex3 atg1* cells, respectively. Hygromycin resistant transformants were selected and correct integration was confirmed by colony PCR with primers TER216 and TER217. The *PEX8-mGFP* fragment was amplified with primers TER234 and TER235 using plasmid pMCE7 (Cepińska et al., 2011) as a template. A fragment encoding *mGFP-PEX8* under the control of the *NOP1* promoter (P_{NOP1}) was amplified with TER306 and TER307 using genomic DNA of strain AK259 as a template. *PEX10-mGFP*, *PEX11-mGFP*, *PEX13-mGFP*, *Ant1-mGFP* fragments were amplified from the yeast GFP fusion library with primers TER218 and TER219, TER222 and TER223, TER226 and TER227, TER299 and TER300, respectively. The above *PEX8-mGFP*, *PEX10*-mGFP, *PEX11-mGFP, PEX13-mGFP*, *Ant1-mGFP*

fragments were transformed into WT and *pex3 atg1* Pex14-mCherry cells. Correct integration was confirmed by colony PCR using primers TER236+TER237, TER220+TER221, TER224+TER225, TER228+
TER229, TER301+TER302, respectively.

Construction of a *TIR1* Pex3-AID*-6HA strain producing Pex14-mGFP and DsRed-SKL

A plasmid encoding Pex3 tagged with the yeast-optimized auxin-inducible degron-6HA tag (AID*-6HA) (Morawska and Ulrich, 2013) was obtained as follows: First, *PEX3* was amplified by PCR using the primers Pex3-F and Pex3-R and *S. cerevisiae* BY4742 genomic DNA as a template. Next, the resulting 1.3kb fragment was digested with *Hin*dIII and *Sal*I, and inserted between the *Hind*III and *Sal*I sites of pHyg-AID*-6xHA, resulting in pHyg-PEX3-AID*-6HA. Then, the *Mfe*1-lineralized pHyg-PEX3-AID*-6HA was integrated in the genome of the *TIR1* strain.

To create a *TIR1* Pex3-AID*-6HA Pex14-mGFP DsRed-SKL strain, the *Dra*I-linearized pPtdh3-DsRed-SKL (Knoops et al., 2015) was transformed into *TIR1* Pex3-AID*-6HA cells. A fragment encoding Pex14-mGFP was amplified with primers TER216 and TER217 using WT Pex14-mGFP (Euroscarf collection) as a template. Then the obtained Pex14-mGFP fragment was transformed into *TIR1* Pex3-AID*-6HA DsRed-SKL cells.

Fluorescence microscopy

All images were captured at room temperature using a 100x1.30 NA Plan Neofluar objective (Carl Zeiss). Images were captured in media in which the cells were grown using a fluorescence microscope (Axio Scope A1; Carl Zeiss), Micro-Manager 1.4 software and a digital camera (Coolsnap HQ2; Photometrics). For wide-field microscopy, GFP

fluorescence was visualized with a 470/40 nm band pass excitation filter, a 495 nm dichromatic mirror, and a 525/50 nm band-pass emission filter. mCherry fluorescence was visualized with a 587/25 nm band pass excitation filter, a 605 nm dichromatic mirror, and a 647/70 nm band-pass emission filter. DsRed fluorescence was visualized with a 546/12 nm bandpass excitation filter, a 560 nm dichromatic mirror, and a 575-640 nm bandpass emission filter. Image analysis was carried out using ImageJ and Adobe Photoshop CS6 software.

To quantify Pex14-mGFP spots in *pex3* and *pex3 atg1* strains, cells were grown for 16 hours on MM-O. Random images were taken as a stack using a confocal microscope (LSM510, Carl Zeiss) and photomultiplier tubes (Hamamatsu Photonics) and Zen 2009 software (Carl Zeiss). Z-Stack images were made containing 14 optical slices and the GFP signal was visualized by excitation with a 488 nm argon ion laser (Lasos), and a 500-550 nm bandpass emission filter.

Live cell imaging was performed using a Zeiss LSM800 confocal microscope. For live cell imaging, the temperature of the objective and object slide was kept at 30°C and the cells were grown on 1% agar in medium. GFP fluorescence was analyzed by excitation of the cell with a 488-nm laser, and emission was detected using a 490 - 535 nm band-pass emission filter. DsRed fluorescence was analyzed by excitation with a 561-nm laser, and emission was detected using a 535 – 700 nm band-pass filter. Eight z-axis planes were acquired every 20 minutes.

Electron microscopy

Cells were fixed in 1.5% $KMnO_4$ and prepared for electron microscopy analysis as described previously (Waterham et al., 1993). Immunocytochemistry was performed using cryosections as described previously (Knoops et al., 2014).

Results

PPVs are present in *S. cerevisiae pex3* and *pex3 atg1* cells

In *H. polymorpha pex3* cells PPVs are very sensitive toward autophagic degradation. This process is prevented by deletion of *ATG1*, which greatly facilitated their identification (Knoops et al., 2014). In order to address whether PPVs are also present in *S. cerevisiae* cells lacking Pex3, we also used an *atg1* background (i.e. an *S. cerevisiae pex3 atg1* double deletion strain). Fluorescence microscopy (FM) analysis of oleic acid induced *pex3 atg1* cells revealed the presence of Pex14-mGFP spots, similar as observed in *H. polymorpha pex3 atg1* cells (**Fig. 1A, B**). However, the number of spots were similar in *S. cerevisiae pex3* and *pex3 atg1* cells, as was evident from quantitative analysis of FM images (**Fig. 1C**). This result indicates that in *S. cerevisiae pex3* cells PPVs are not subject to constitutive degradation by autophagy. This was confirmed by Western blot analysis, which showed that the levels of Pex14 in *pex3* cells were comparable to those in wild-type (WT) and *pex3 atg1* cells (**Fig. 1E**).

In order to address whether the observed Pex14-mGFP spots in *S. cerevisiae pex3 atg1* cells indeed represent PPVs, we performed immuno electron microscopy (iEM) analysis using α-Pex14 antibodies. These experiments revealed that *S. cerevisiae pex3 atg1* cells contain clusters of vesicular structures (**Fig. 1D**), which are selectively labeled with α-Pex14 antibodies, indicating that they are peroxisomal in nature.

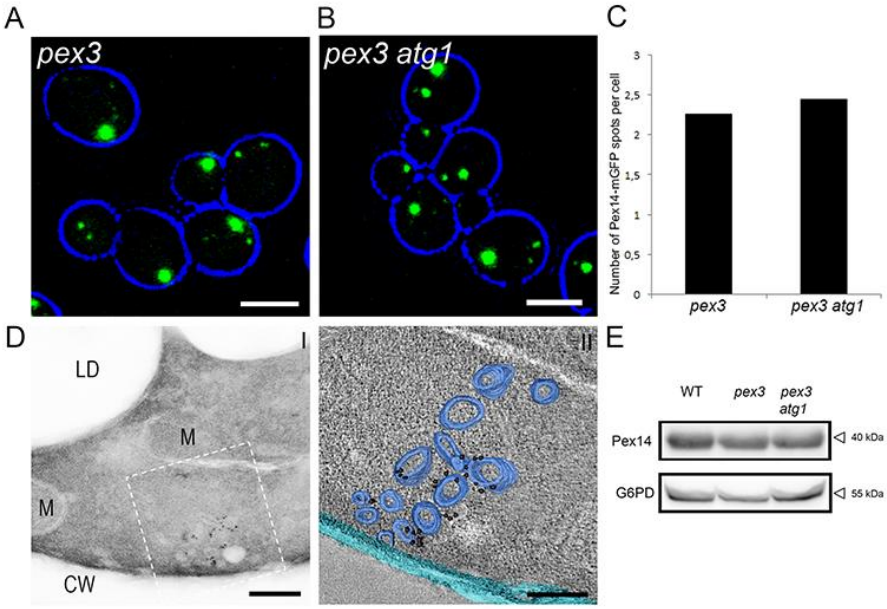

Figure 1. PPVs are present in oleic acid induced *S. cerevisiae pex3* and *pex3 atg1* cells.

Cells were grown on a mixture of glucose and oleic acid for 16 h. FM images of *pex3* **(A)** and *pex3 atg1* **(B)** cells producing Pex14-mGFP. Scale bar: 2.5 µm. **(C)** Quantification of Pex14-mGFP spots in *pex3* and *pex3 atg1* cells. The average number of spots was calculated from 200 cells in each strain. (**D**) I. Immuno-electron microscopy analysis of *pex3 atg1* cells. Labelling was performed on a 90 nm thick cryosection using anti-Pex14 antibodies. II shows a 3D reconstruction of a dual tilt tomogram of the 90 nm thick section selected in I. PPVs (blue), plasma membrane (magenta). Scale bars: D I - 200 nm, D II - 100 nm. M – mitochondrion, LD-lipid droplet; CW – cell wall. (E) Western blot analysis of Pex14 levels in WT, *pex3* and *pex3 atg1* cells. G6PD was used as loading control.

PPVs in *S. cerevisiae pex3 atg1* cells contain Pex14 and Pex8

In order to address whether the PPVs in *S. cerevisiae pex3 atg1* cells have a similar protein composition as in *H. polymorpha pex3 atg1* cells, we performed co-localization

studies using Pex14-mCherry together with different PMPs C-terminally tagged with mGFP under control of their endogenous promoters. As expected the PMPs Pex10-GFP, Pex11-GFP and Ant1-GFP were present in spots in WT control cells (**Fig. 2A**). Pex8-GFP, however, was partially mislocalized to the cytosol in WT controls (**Fig. 2A**). We therefore also tested the localization of a Pex8 variant which was N-terminally tagged with mGFP and produced under the control of P_{NOP1} (Yofe et al., 2016). As shown in **Fig. 2A**, GFP-Pex8 was confined to spots in WT cells, indicating that the C-terminal GFP tag influenced the peroxisomal localization of Pex8.

As shown in Fig. 2B, in *S. cerevisiae pex3 atg1* cells bulk of the GFP-Pex8 fluorescence co-localized with Pex14-mCherry in spots (**Fig. 2B**), indicating that Pex8 associates with PPVs, like in *H. polymorpha pex3 atg1*. In contrast, Pex10-mGFP, Pex13-mGFP and Ant1-mGFP fluorescence was below the limit of detection in *pex3 atg1* cells (data not shown). The reduced levels of these PMPs, but not of Pex14, was confirmed by Western blot analysis (**Fig. 2C**). Pex11-mGFP fluorescence was present in foci, which did not co-localize with Pex14-mCherry (**Fig. 2B**). Further analysis, using live cell imaging and mitotracker staining, revealed that Pex11-GFP localized to mitochondria in *pex3 atg1* cells (**Fig. 2D**). The levels of Pex11 were strongly reduced in *pex3 atg1* cells relative to WT controls, indicating that this peroxin is also relatively unstable in these cells (**Fig. 2C**).

Taken together, we conclude that Pex14 and Pex8, but not Pex10, Pex11, Pex13 and Ant1 associate with PPVs in *S. cerevisiae pex3 atg1* cells.

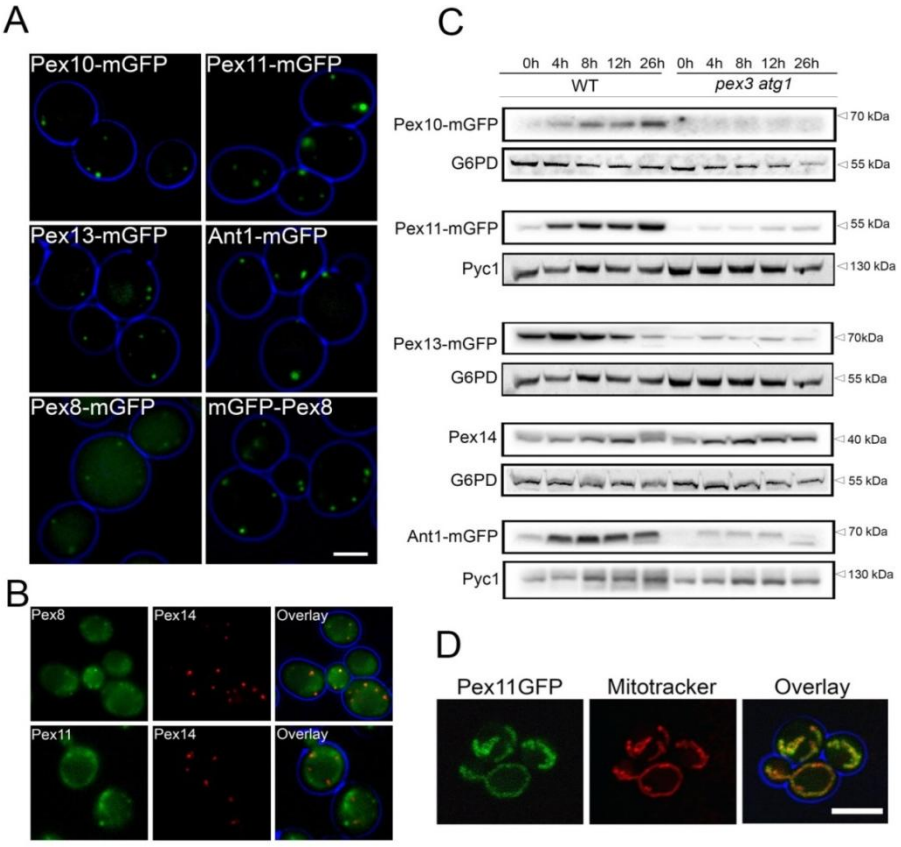

Figure 2 PMPs levels and localization in *pex3 atg1* cells. (A) FM analysis of glucose grown WT cells producing various PMPs fused to mGFP. Scale bar: 2.5 µm. **(B)** FM analysis of glucose grown *pex3 atg1* producing Pex14-mCherry together with different PMPs fused with mGFP. **(C)** Western blot analysis of the levels of Pex10, Pex11, Pex13, Pex14, Ant1 in *S. cerevisiae* WT and *pex3 atg1* cells. Cells were grown in mineral medium containing glucose, subsequently shifted to mineral medium containing a mixture of glucose and oleic acid. TCA samples were taken at the indicated time points. Pyc1 or G6PD were used as loading controls. (**D**) Confocal laser scanning microscopy analysis of *pex3 atg1* cells producing Pex11-mGFP. Mitochondria were stained with Mitotracker (Red). In order to improve visualization of mitochondria, cells growing on glucose medium containing 1% agar were imaged. Scale bar: 5 µm.

S. cerevisiae PPVs mature into functional peroxisomes upon reintroduction of Pex3

In order to investigate whether PPVs can develop into functional peroxisomes upon reintroduction of Pex3, we used an auxin-inducible degron system (Kanke et al., 2011; Morawska and Ulrich, 2013; Nishimura et al., 2009) for modulating Pex3 levels in a strain producing Pex14-mGFP and the peroxisomal matrix marker DsRed-SKL.

In this strain Pex3, produced under control of its endogenous promoter, is continuously degraded in cultures containing auxin, but is stable in the absence of auxin. The advantage of this system is that, unlike using inducible, strong promoters such as $P_{GAL,}$ Pex3 is never overproduced.

As expected, the peroxisomal matrix marker DsRed-SKL is cytosolic when cells were grown in the presence of auxin (Fig. 3A). However, several hours after removing auxin DsRed-SKL co-localized with Pex14-mGFP, indicating that the PPVs became competent to import matrix proteins. This was confirmed by live cell imaging (**Fig. 3B**). Taken together these data indicate that PPVs can develop into functional peroxisomes when Pex3 protein is reintroduced in the cells.

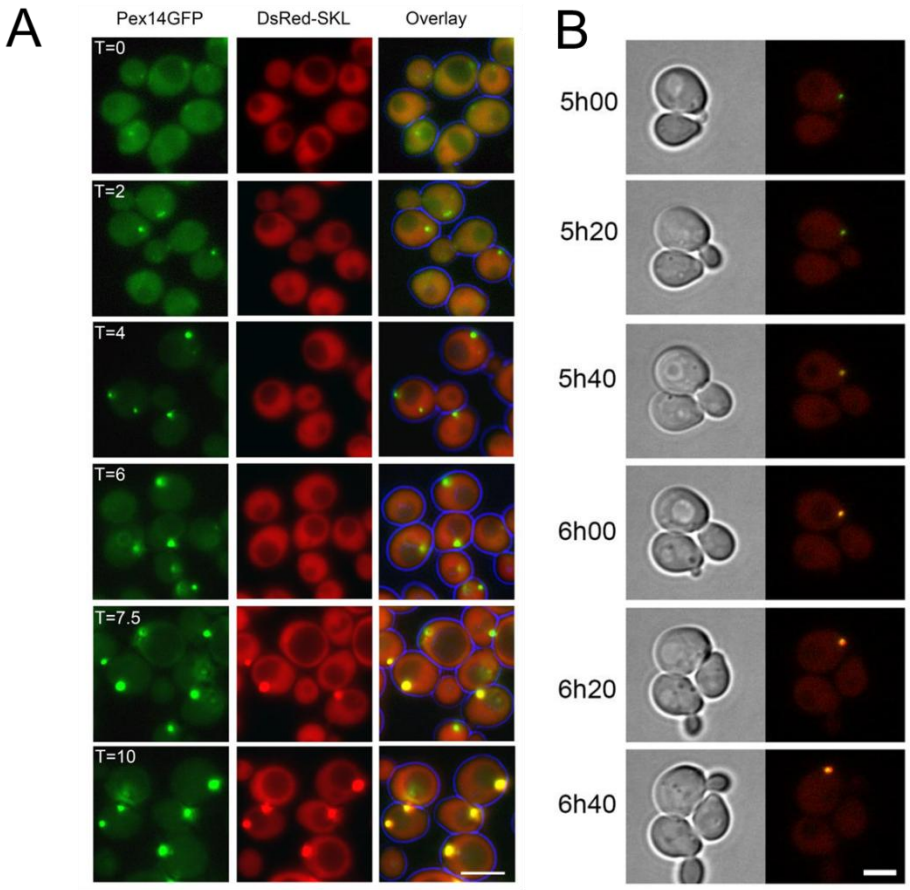

Figure 3. Reintroduction of Pex3 results in import of DsRed-SKL in PPVs. (A) *S. cerevisae* Pex3-AID*-6HA Pex14-mGFP DsRed-SKL cells were precultivated on glucose medium in the presence of auxin. At T = 0h, cells were transferred to fresh glucose medium without lacking auxin. FM analysis shows that at T = 0h all DsRed mislocalizes to the cytosol, whereas several hours after the shift (T = 7.5 h) DsRed-SKL also co-localized with Pex14-mCherry. (B) Live cell imaging showing reintroduction of peroxisomes in *S. cerevisae* Pex3-AID*-6HA Pex14-mGFP DsRed-SKL cells upon removal of auxin. Scale bar: 2.5 µm.

Discussion

We demonstrated that *Saccharomyces cerevisiae* cells lacking Pex3, which until now were considered to lack any peroxisomal membrane structures, in fact do contain such membranes (pre-peroxisomal vesicles, PPVs). Like in *H. polymorpha* these membrane structures harbored Pex14 and Pex8, but not the RING protein Pex10 or Ant1, which were both below the limit of detection.

The PPVs in *S. cerevisiae pex3* cells differ from those in *H. polymorpha pex3* cells in three aspects. First, they are relatively stable whereas those in *H. polymorpha pex3* cells are subject to constitutive autophagic degradation (Knoops et al., 2014). Second, Pex13 does not accumulate on the PPVs in *S. cerevisiae pex3 atg1* cells. Third, Pex11 localizes to mitochondria in *S. cerevisiae pex3 atg1* cells, whereas this peroxin was present at the ER in *H. polymorpha pex3 atg1* cells. This difference in location in the two organisms suggests that Pex11 mislocalizes in the absence of Pex3. Importantly, as in *H. polymorpha*, also the PPVs in *S. cerevisiae* cells lacking Pex3, matured into normal peroxisomes upon reintroduction of Pex3. This indicates that the ER-based *de novo* peroxisome formation pathway proposed by van der Zand et al. (2012) needs adaptation.

The remarkable difference between the stability of PPVs in *S. cerevisiae* and *H. polymorpha* can be readily explained by the difference in function of Pex3 protein in pexophagy in the two organisms. In *S. cerevisiae* Pex3 is required for pexophagy (Motley et al., 2012), whereas in *H. polymorpha* Pex3 should be absent on peroxisomes to allow pexophagy (Bellu et al., 2002) thus explaining why PPVs lacking Pex3 are sensitive to autophagic degradation in the latter organism.

Previously, in *S. cerevisiae pex3* cells, 15 PMPs were reported to be localized to the ER, including Pex8, Pex11, Pex13,

Pex14 and Atn1(van der Zand et al., 2010). In this study a C-terminal YFP fusion protein of Pex8 was used. Here we show that Pex8-mGFP partially mislocalizes to the cytosol in WT cells. Most likely, this is due to the presence of peroxisomal targeting signal 1 (PTS1) at C-terminus of Pex8 (Rehling et al., 2000), which upon addition of a fluorescent protein causes partial mis-localization. Indeed, when we fused GFP to the N-terminus of Pex8 no cytosolic GFP was detected in WT cells. In *S. cerevisiae pex3 atg1* GFP-Pex8 was predominantly associated with PPVs as it co-localized with Pex14-mCherry.

In *S. cerevisiae pex3* cells Pex11 has been reported to be either mislocalized to the cytosol, the ER, or mitochondria (Hettema et al., 2000; van der Zand et al., 2010; Mattiazzi Ušaj et al., 2015, Motley et al., 2015). Using Western blot analysis, Hettema et al.(2000) showed that the levels of Pex11 are very low in *S. cerevisiae pex3* cells. Immunofluorescence revealed a weak and diffuse staining, whereas immunolabelling did not reveal the association of Pex11-HA to membrane structures, suggesting that the protein was cytosolic (Hettema et al., 2000). In contrast, van der Zand and colleagues (2010) localized Pex11-YFP to the ER in *S. cerevisiae pex3* cells. Recently, however, two groups showed that Pex11-GFP was localized to mitochondria in *S. cerevisiae pex3* cells (Mattiazzi Ušaj et al., 2015; Motley et al., 2015). The latter observation is fully in line with our current data. We also observed a significant decrease in total Pex11 levels in the cells lacking Pex3, relative to the WT control. Our data that PPVs contain at least Pex14 and Pex8 challenges the view that all PMPs sort to the ER before routing to the target peroxisome (van der Zand et al., 2010). Moreover, it also opposes the assumption that all PMPs follow a similar pathway to peroxisomes as the PPVs contain specific PMPs that are sorted to these structures without the ER as intermediate.

Until recently, it was generally accepted that cells lacking Pex3 lack peroxisomal membrane remnants. The finding that

yeast *pex3* cells harbor PPVs that can develop into functional peroxisomes upon Pex3 re-introduction lends us to support the view that the current *de novo* model that peroxisomes arise from the ER is no longer generally valid. In fact, our data support the view that in all *pex* mutants known so far new organelles arise from pre-existing peroxisomal membrane vesicles. Hence, studies on *de novo* peroxisome biosynthesis require other models that lack these remnants structures, for instance yeast mutant cells that are affected in organelle inheritance.

Table 1. strains used in this study

WT	BY4742, MATα his3Δ1 leu2Δ0 lys2Δ0 ura3Δ0	Euroscarf
TIR1	DF5, ADH1-AtTIR1^{9myc}::*URA3*	(Morawska and Ulrich, 2013)
pex3	BY4742, *PEX3*::*KanMX*	Euroscarf
pex3 atg1	BY4742, *PEX3*::*KanMX*, *ATG1*::*NAT*	This study
*pex*3 Pex14-mGFP	BY4742, *PEX3*::*KanMX*, Pex14-mGFP:: *HIS3*	This study
*pex*3 *atg1* Pex14-mGFP	BY4742, *PEX3*::*KanMX*, *ATG1*::*NAT*, Pex14-mGFP::*HIS3*	This study
WT Pex8-mGFP	BY4742, Pex8-mGFP::*HIS3*	This study
WT Pex10-mGFP	BY4742, Pex10-mGFP::*HIS3*	This study
WT Pex11-mGFP	BY4742, Pex11-mGFP::*HIS3*	This study
WT Pex13-mGFP	BY4742, Pex13-mGFP::*HIS3*	This study
WT Ant1-mGFP	BY4742, Ant1-mGFP::*HIS3*	This study
WT Pex14-mCherry P_{NOP1}GFP-Pex8	BY4742, Pex14-mCherry::*HPH* P_{NOP1}GFP-Pex8::*URA3*	This study
AK259	BY4742, *PEX3*::*KanMX*, *ATG1*::*NAT*, Pex14-mCherry::*HPH* P_{NOP1}mGFP-Pex8::*URA3*	(Agrawal et al., 2016)
pex3 atg1 Pex14-mCherry Pex10-mGFP	BY4742, *PEX3*::*KanMX*, *ATG1*::*NAT,* Pex14-mCherry::*HPH,* Pex10-mGFP::*HIS3*	This study
pex3 atg1 Pex14-	BY4742, *PEX3*::*KanMX*,	This study

mCherry Pex11-mGFP	*ATG1*::*NAT,* Pex14-mCherry::*HPH,* Pex11-mGFP::*HIS3*	
pex3 atg1 Pex14 -mCherry Pex13-mGFP	BY4742, *PEX3*::*KanMX*, *ATG1*::*NAT,* Pex14-mCherry::*HPH,* Pex13-mGFP::*HIS3*	This study
pex3 atg1 Pex14 -mCherry Ant1-mGFP	BY4742, *PEX3*::*KanMX*, *ATG1*::*NAT,* Pex14-mCherry::*HPH,* Ant1-mGFP::*HIS3*	This study
pex3 atg1 Pex11-mGFP	BY4742, *PEX3*::*KanMX*, *ATG1*::*NAT,* Pex11-mGFP::*HIS3*	This study
Pex3-AID*-6HA	DF5,ADH1-AtTIR1^{9myc}:: *URA3,*pHyg-PEX3-AID*-6HA: : *HPH*	This study
Pex3-AID*-6HA Pex14-mGFP DsRed-SKL	DF5,ADH1-AtTIR1^{9myc}::*URA3* , Pex14-mGFP::*HIS3,* pHyg-PEX3-AID*-6HA:: *HPH*, P_{TDH3}-DsRed-SKL::*LEU2*	This study

Table 2. Oligonucleotides used in this study (5' to 3')

TER198	TGCATGGATCAGACGCTTTC
TER199	AATGGGCCAATAGCAAGGAG
TER202	CAAGTAGTAGAGTTTGCGTG
TER203	ATCGCTGCAGGGTAATGTCA
TER208	ACCCCATATTTTCAAATCTCTTTTACAACACCAGACGAG AAATTAAGAAACCAGATCTGTTTAGCTTGCCTT
TER209	ATAGCAGGTCATTTGTACTTAATAAGAAAACCATATTAT GCATCACTTAAATTCGAGCTCGTTTTCGACA
TER295	AGATCAGTGTCCCTGACTGGCAAAATGGACAGGTCGA AGACTCCATCCCAGTATCACCCGGGAAATACCCA
TER296	GTTACAATTACAATTTCCGTTAAAAAACTAATTACTTAC ATAGAATTGCG TGCGTACACGCGTCTGTACA
TER214	AGATCAGTGTCCCTGACTGGCAAAATGGACAGGTCGA AGACTCCATCCCAATGGTGAGCAAGGGCGAGGAGGAT
TER215	GTTACAATTACAATTTCCGTTAAAAAACTAATTACTTAC ATAGAATTGCGCGTTTTCGACACTGGATGGCGGCGTT
TER216	TAACCGTATGGAATCCGGTA
TER217	TCCATGGCAATTCAAGGTCAT
TER234	CCATCGACTGGTGGTACACAACGGTCTTATCAAGTCAA TCTTCTAAATTA-GTGAGCAAGGGCGAGGAGCTGTT
TER235	TTGAGAAAAAAGGAATATAAAAAGGCGCTACTATAAAG TACTTAATGATA-GAACTAGTGGATCCCCCGTA
TER236	AGCATTTGCTTAGGGACTCT
TER237	TGAAGGGGGGTATCTTTGGA
TER306	GACTAGAATCCCGGACTTGG
TER307	GATTGAACTGGTCAAGCAACT
TER218	TACTAGGTCGTCTGTTGGTC
TER219	ACTACCTCCACCAAAGCCAA
TER220	TAGACGTACACATGACCCTC
TER221	ACACTCTGAGACCCGTGCAA
TER222	AGTGGTCTGGCTATGGATCT
TER223	TATCACGAGCGGGTAACAGA

TER224	ACTTGCAGGCAGCTGCTAAA
TER225	CCCTGAAATATATAGGCGCA
TER226	AGACCTCTGGAACCATACGA
TER227	TGCCATATCACAATTGTCCTGA
TER228	TGATAGGCGCTGTTACTGGA
TER229	GGTGCTGGTAAGAAGAAAGT
TER299	GGGTGTCCTTTCCAAGATGA
TER300	TCCCAATTCCAAGTGGCTCT
TER301	GTGGTAGCTACAAGACAACA
TER302	GACCTGCGTTGAAGTGGAAC
Pex3-F	CCCAAGCTTTTGACGGCATACACCCAAGA
Pex3-R	AGAGTCGACAGGCTTGAAGGAAAACGAGC

References

1. Agrawal G., S.N. Fassas, Z.J, Xia, S.Subramani. Distinct requirements for intra-ER sorting and budding of peroxisomal membrane proteins from the ER. J. Cell Biol. 212:335-348.
2. Baerends, R.J., K.N. Faber, A.M. Kram, J.A. Kiel, I.J. van der Klei, and M. Veenhuis. 2000. A stretch of positively charged amino acids at the N terminus of Hansenula polymorpha Pex3p is involved in incorporation of the protein into the peroxisomal membrane. J. Biol. Chem. 275:9986–9995.

3. Bellu, A.R., F.A. Salomons, J.A.K.W. Kiel, M. Veenhuis, and I.J. van der Klei. 2002. Removal of Pex3p Is an Important Initial Stage in Selective Peroxisome Degradation in Hansenula polymorpha. J. Biol. Chem. 277:42875–42880.

4. van den Bosch, H., R.B. Schutgens, R.J. Wanders, and J.M. Tager. 1992. Biochemistry of peroxisomes. Annu. Rev. Biochem. 61:157–197.

5. Cepińska, M.N., M. Veenhuis, I.J. van der Klei, and S. Nagotu. 2011. Peroxisome fission is associated with reorganization of specific membrane proteins. Traffic Cph. Den. 12:925–937.

6. Goldstein, A.L., and J.H. McCusker. 1999. Three new dominant drug resistance cassettes for gene disruption in Saccharomyces cerevisiae. Yeast Chichester Engl. 15:1541–1553.

7. Grimm, I., D. Saffian, H.W. Platta, and R. Erdmann. 2012. The AAA-type ATPases Pex1p and Pex6p and their role in peroxisomal matrix protein import in Saccharomyces cerevisiae. Biochim. Biophys. Acta. 1823:150–158.
8. Hettema, E.H., W. Girzalsky, M. van Den Berg, R. Erdmann, and B. Distel. 2000. Saccharomyces cerevisiae pex3p and pex19p are

required for proper localization and stability of peroxisomal membrane proteins. EMBO J. 19:223–233.

9. Hoepfner, D., D. Schildknegt, I. Braakman, P. Philippsen, and H.F. Tabak. 2005. Contribution of the Endoplasmic Reticulum to Peroxisome Formation. Cell. 122:85–95.

10. Honsho, M., S. Yamashita, and Y. Fujiki. Peroxisome homeostasis: Mechanisms of division and selective degradation of peroxisomes in mammals. Biochim. Biophys. Acta BBA - Mol. Cell Res.

11. Janke, C., M.M. Magiera, N. Rathfelder, C. Taxis, S. Reber, H. Maekawa, A. Moreno-Borchart, G. Doenges, E. Schwob, E. Schiebel, and M. Knop. 2004. A versatile toolbox for PCR-based tagging of yeast genes: new fluorescent proteins, more markers and promoter substitution cassettes. Yeast Chichester Engl. 21:947–962.

12. Kanke, M., K. Nishimura, M. Kanemaki, T. Kakimoto, T.S. Takahashi, T. Nakagawa, and H. Masukata. 2011. Auxin-inducible protein depletion system in fission yeast. BMC Cell Biol. 12:8.

13. Knoops, K., R. de Boer, A. Kram, and I.J. van der Klei. 2015. Yeast pex1 cells contain peroxisomal ghosts that import matrix proteins upon reintroduction of Pex1. J. Cell Biol. 211:955–962.

14. Knoops, K., S. Manivannan, M.N. Cepińska, A.M. Krikken, A.M. Kram, M. Veenhuis, and I.J. van der Klei. 2014. Preperoxisomal vesicles can form in the absence of Pex3. J. Cell Biol. 204:659–668.
15. Kumar, S., R. Singh, C.P. Williams, and I.J. van der Klei. Stress exposure results in increased peroxisomal levels of yeast Pnc1 and Gpd1, which are imported via a piggy-backing mechanism. Biochim. Biophys. Acta BBA - Mol. Cell Res.

16. Lam, S.K., N. Yoda, and R. Schekman. 2011. A vesicle carrier that mediates peroxisome protein traffic from the endoplasmic reticulum. Proc. Natl. Acad. Sci. U. S. A. 108:E51–52.

17. Lazarow, P.B., and Y. Fujiki. 1985. Biogenesis of Peroxisomes. Annu. Rev. Cell Biol. 1:489–530.

18. Manivannan, S., R. de Boer, M. Veenhuis, and I.J. van der Klei. 2013. Lumenal peroxisomal protein aggregates are removed by concerted fission and autophagy events. Autophagy. 9:1044–1056.

19. Mast, F.D., R.A. Rachubinski, and J.D. Aitchison. 2015. Signaling dynamics and peroxisomes. Curr. Opin. Cell Biol. 35:131–136.

20. Mattiazzi Ušaj, M., M. Brložnik, P. Kaferle, M. Žitnik, H. Wolinski, F. Leitner, S.D. Kohlwein, B. Zupan, and U. Petrovič. 2015. Genome-Wide Localization Study of Yeast Pex11 Identifies Peroxisome-Mitochondria Interactions through the ERMES Complex. J. Mol. Biol.

21. Morawska, M., and H.D. Ulrich. 2013. An expanded tool kit for the auxin-inducible degron system in budding yeast. Yeast Chichester Engl. 30:341–351. doi:10.1002/yea.2967.

22. Motley, A.M., P.C. Galvin, L. Ekal, J.M. Nuttall, and E.H. Hettema. 2015. Reevaluation of the role of Pex1 and dynamin-related proteins in peroxisome membrane biogenesis. J. Cell Biol. 211:1041–1056.
23. Motley, A.M., J.M. Nuttall, and E.H. Hettema. 2012. Pex3-anchored Atg36 tags peroxisomes for degradation in Saccharomyces cerevisiae. EMBO J. 31:2852–2868.

24. Motley, A.M., G.P. Ward, and E.H. Hettema. 2008. Dnm1p-dependent peroxisome fission requires Caf4p, Mdv1p and Fis1p. J. Cell Sci. 121:1633–1640.

25. Nishimura, K., T. Fukagawa, H. Takisawa, T. Kakimoto, and M. Kanemaki. 2009. An auxin-based degron system for the rapid depletion of proteins in nonplant cells. Nat. Methods. 6:917–922.

26. Opaliński, Ł., J.A.K.W. Kiel, C. Williams, M. Veenhuis, and I.J. van der Klei. 2011. Membrane curvature during peroxisome fission requires Pex11. EMBO J. 30:5–16.

27. Rehling, P., A. Skaletz-Rorowski, W. Girzalsky, T. Voorn-Brouwer, M.M. Franse, B. Distel, M. Veenhuis, W.-H. Kunau, and R. Erdmann. 2000. Pex8p, an Intraperoxisomal Peroxin of Saccharomyces cerevisiae Required for Protein Transport into Peroxisomes Binds the PTS1 Receptor Pex5p. J. Biol. Chem. 275:3593–3602.

28. Saraya, R., A.M. Krikken, J.A.K.W. Kiel, R.J.S. Baerends, M. Veenhuis, and I.J. van der Klei. 2012. Novel genetic tools for Hansenula polymorpha. FEMS Yeast Res. 12:271–278.

29. Smith, J.J., and J.D. Aitchison. 2013. Peroxisomes take shape. Nat. Rev. Mol. Cell Biol. 14:803–817.

30. Tabak, H.F., I. Braakman, and A. van der Zand. 2013. Peroxisome formation and maintenance are dependent on the endoplasmic reticulum. Annu. Rev. Biochem. 82:723–744.
31. Tabak, H.F., A. van der Zand, and I. Braakman. 2008. Peroxisomes: minted by the ER. Curr. Opin. Cell Biol. 20:393–400.

32. van der Zand, A., J. Gent, I. Braakman, and H.F. Tabak. 2012. Biochemically Distinct Vesicles from the Endoplasmic Reticulum Fuse to Form Peroxisomes. Cell. 149:397–409.

33. Waterham, H.R., V.I. Titorenko, G.J. Swaving, W. Harder, and M. Veenhuis. 1993. Peroxisomes in the methylotrophic yeast Hansenula

polymorpha do not necessarily derive from pre-existing organelles. EMBO J. 12:4785–4794.

34. Williams, C., L. Opalinski, C. Landgraf, J. Costello, M. Schrader, A.M. Krikken, K. Knoops, A.M. Kram, R. Volkmer, and I.J. van der Klei. 2015. The membrane remodeling protein Pex11p activates the GTPase Dnm1p during peroxisomal fission. Proc. Natl. Acad. Sci. 112:6377–6382.

35. van der Zand, A., I. Braakman, and H.F. Tabak. 2010. Peroxisomal membrane proteins insert into the endoplasmic reticulum. Mol. Biol. Cell. 21:2057–2065.

36. U. Weill, M. Meurer, S. Churtzman, E. Zalckvar, O, Goldman, S. Be-Dor, C. S. Schütze, N. Wiedemann, M. Knoop, A. Khmelinskii, M.Schuldiner. One library to make them all: streamlining the creation of yeast libraries via a SWAp-Tag strategy. *Nat Methods*. 13:371-378.